Article ID: 1000-324X(2022)04-0459-08 **DOI:** 10.15541/jim20210230

Porous SiC Ceramic Matrix Composite Reinforced by SiC Nanowires with High Strength and Low Thermal Conductivity

RUAN Jing[1,2,3], YANG Jinshan[1,2], YAN Jingyi[1,2,4], YOU Xiao[1,2,4], WANG Mengmeng[1,2,4], HU Jianbao[1,2], ZHANG Xiangyu[1,2], DING Yusheng[1,2], DONG Shaoming[1,2,5]

(1. State Key Laboratory of High Performance Ceramics & Superfine Microstructure, Shanghai Institute of Ceramics, Chinese Academy of Sciences, Shanghai 200050, China; 2. Structural Ceramics and Composites Engineering Research Center, Shanghai Institute of Ceramics, Chinese Academy of Sciences, Shanghai 201899, China; 3. School of Physical Science and Technology, ShanghaiTech University, Shanghai 201210, China; 4. University of Chinese Academy of Sciences, Beijing 100039, China; 5. Center of Materials Science and Optoelectronics Engineering, University of Chinese Academy of Sciences, Beijing 100049, China)

Abstract: Porous design of SiC composites with lightweight, high strength and low thermal conductivity can be obtained by constructing porous silicon carbide nanowires (SiCNWs) network and controlling chemical vapor infiltration (CVI) process. The SiCNWs network with an optimized volume fraction (15.6%) and uniform pore structure was prepared by mixing SiCNWs and polyvinyl alcohol (PVA) firstly. SiCNWs reinforced porous SiC ceramic matrix composite (SiCNWs/SiC) with a small uniform pore can be obtained by controlling the CVI parameters. The morphology of the grown SiC matrix, from the spherical particles to the hexagonal pyramid particles, can be influenced by the CVI parameters, such as temperature and reactive gas concentration. The strength of the SiCNWs/SiC ceramic matrix composites reaches (194.3±21.3) MPa with a porosity of 38.9% and thermal conductivity of (1.9± 0.1) W/(m·K), which shows the toughening effect and low thermal conductivity design.

Key words: SiC ceramic matrix composite; silicon carbide nanowire; CVI parameter; porosity; thermal conductivity

The temperature of the hypersonic vehicle rises due to the violent friction between the outer wall and the air, while its internal components require a relatively low and stable temperature. To realize the lightweight and low heat transfer efficiency, porous material with inherently half-closed pores can effectively hinder the convective heat transfer of the gas and consequently reduce the thermal conductivity[1]. Porous ceramics are relatively high-quality porous material for their lightweight, high-temperature resistance, and excellent chemical corrosion resistance performance, which can be widely used in various extreme environments[2-6]. However, the pore structure shows a negative influence on the mechanical strength of the porous ceramics[7-8], in which the brittle failure can be regarded as the major obstacle in its practical application. For the improvement of brittleness, the introduction of reinforcements can be applied to toughen ceramics and may have a positive effect on the toughness of the material. SiC fibers have been used as the reinforcements of composites for their excellent performance[9-10]. SiCNWs possess superior physical and chemical properties as compared with the traditional SiC fibers, and the mechanical strength of SiCNWs is an order of magnitude higher than that of SiC fibers[11-13]. So SiCNWs can be considered as a new reinforcement to replace SiC fibers to improve the bonding strength between the pore walls for their excellent performance.

A marked risen in the elastic modulus (up to 90%) has been reported even with the addition of a small quantity (0.8% (volume percent)) of nanowires[14]. The yield strength of SiCNWs/Al composites can be improved by optimizing the content of SiCNWs of 15%, 20%, and 25% (volume percent)[15]. As long as SiCNWs grow on carbon fiber, the interlaminar shear strength of SiCNWs-C/C composites can be enhanced

Received date: 2021-04-07; **Revised date:** 2021-06-27; **Published online:** 2021-06-30
Foundation item: National Natural Science Foundation of China (51772310); Chinese Academy of Sciences Key Research Program of Frontier Sciences (QYZDY-SSWJSC031); Innovation Academy for Light-duty Gas Turbine, Chinese Academy of Sciences (CXYJJ20-MS-02)
Biography: RUAN Jing (1993–), male, PhD candidate. E-mail: ruanjing@shanghaitech.edu.cn
阮 景(1993–), 男, 博士研究生. E-mail: ruanjing@shanghaitech.edu.cn
Corresponding author: YANG Jinshan, professor. E-mail: jyang@mail.sic.ac.cn; DONG Shaoming, professor. E-mail: smdong@.sic.ac.cn
杨金山, 研究员. E-mail: jyang@mail.sic.ac.cn; 董绍明, 研究员. E-mail: smdong@mail.sic.ac.cn

by 32% as compared with the baseline[16]. The addition of the reinforcing phase can improve the strength of porous ceramic, but the strength of porous ceramic is more sensitive to pore size. Staggered one-dimensional nanowires are expected to build many nanopores, and toughen effect can be realized by reducing the size of the pore[17-19]. The low thermal conductivity of air fills the pores and the small size of pores causes less damage to mechanical strength, which makes it a better insulation effect, and possibly existing SiCNWs- pullout is expected to improve the brittleness[20]. At present, the introduction of SiCNWs into composite materials is usually based on the *in-situ* growth method[21-23], and the purity and quality of the introduced SiCNWs are difficult to be controlled. Traditional porous ceramic sintering methods are not suitable for SiCNWs applied in composite, grinding and sintering will destroy nanowire structure[24-25]. SiCNWs are hard to be woven like SiC fibers, so it is difficult to prepare a porous SiCNWs network.

In this work, SiCNWs and PVA are mixed to form and fix the SiCNWs network, and the volume fraction and pore structure parameters of the SiCNWs network are controlled by adjusting the ratio of SiCNWs to PVA. The one-dimensional nanostructure of SiCNWs is used to construct a complex and porous network skeleton by controlling CVI parameters to change chemical reaction dynamics. Besides, combining morphology and pore parameters, the influence of different reaction environments on the pore structure is discussed in detail[26-27].

1 Experimental Procedure

1.1 Preparation of SiCNWs dispersion and network skeleton

Homogenous dispersed SiCNWs (about 10 μm in length and 120 nm in diameter) solution was prepared firstly by mixing SiCNWs (Changsha Sinet Advanced Materials Co., Ltd., China) and dispersant polyvinylpyrrolidone (PVP, Hangzhou Weitong Nanometer Material Co., Ltd., China) in deionized water by sonication (Ningbo Xinzhi Biotechnology Co., Ltd., China) at 300 W for 100 min. The weight ratio of SiCNWs to PVP to water was controlled at 6∶1∶200. Then, PVA dispersant was added to disperse SiCNWs with *w*(PVA)∶*w*(SiCNWs)=1.3∶1. After that, the semidry SiCNWs/PVA mixture was poured into the mold to prepare a film with a size of 30 mm×30 mm×0.7 mm, and the SiCNWs formed a network when the solvent was completely evaporated.

1.2 Preparation of PyC interphase and SiCNWs/SiC ceramic matrix composites

Before the deposition of the SiC matrix, the SiCNWs/PVA film was put into a tube furnace for degumming and pyrolytic carbon (PyC) interphase preparation. PVA and PVP were completely removed after 60 min of pyrolysis at 800 ℃ and a complete SiCNWs network was formed in the tube furnace. CVI process was applied to prepare PyC interphase by the pyrolysis of CH_4[28]. The flow ratio of CH_4 was controlled at 50 sccm at 3 kPa for several minutes.The SiC matrix was introduced into the SiCNWs network by pyrogenic decomposition of methyltrichlorosilane (MTS, CH_3SiCl_3) as the gaseous precursor, and hydrogen (H_2) was selected as carrier and dilution gas of MTS. The flow ratio of carrier H_2 is 200 sccm and dilute H_2 is 60 sccm, and the whole pressure of the deposition reaction was controlled at 3 kPa for several hours. The morphology of the deposited SiC matrix and pore size are influenced by the reaction parameters.

1.3 Characterization

The surface and internal morphology of the samples were characterized by scanning electron microscope (SEM; Hitachi SU8220, Japan). The biaxial bending strength was tested by universal material testing machine (UTM, Zhejiang Zili Co., Ltd. Zhejiang, China), in which the samples were prepared into small flat discs with a diameter of 16 mm. The discs were placed on three fixed spheres and formed an equilateral triangle with a side length of 7 mm. The pore parameters were tested by a mercury porosimeter (Micromeritics Instrument Co (Shanghai)., Ltd, America). The porosity of samples throughout the CVI process must be strictly analyzed, which reflects the change of the structure and pore size during the *in-situ* growth of the SiC matrix. Thermal diffusivity of the SiCNWs/SiC ceramic matrix composite with a size of 12.6 mm in diameter and 0.7 mm in thickness was tested under a laser thermal instrument (Laser thermal conductivity meter, TD-79A) from room temperature to 500 ℃ at a step of 50 ℃. The sample was ground into micron-sized powder and filled a container with a diameter of 5 mm and a height of 18 mm for specific heat test (MHTC96, Oriental Scientific Instruments Shanghai Import and Export Co., Ltd., France).

2 Results and discussion

Fig. 1 shows the morphologies of the SiCNWs net-

work before and after deposition of the SiC matrix. Fig. 1(a) is the surface morphology of the SiCNWs/PVA film, it shows that SiCNWs are completely wrapped by PVA. Fig. 1(b) is the original SiCNWs network skeleton, which shows various shapes of SiCNWs and some bulges like fish scales can be found on the nanowire. Fig. 1(c, d) are the surface morphologies of the SiCNWs/SiC ceramic matrix composites with a small amount of deposited SiC. The porosity of Fig. 1(c, d) is 87.1% and 84.2%, respectively. The SiCNWs can be found wrapped in SiC matrix without interphase, as shown in Fig. 1(c). Differently, the grown SiC matrix aggregates into clusters and shows the state of lumpy particles around SiCNWs with PyC interphase as shown in Fig. 1(d). SiC matrix deposits unevenly on the PyC interphase, which can be attributed to the weak and unstable bonding strength of SiC and PyC, and consequently the bonding energy of SiC and PyC is higher than that of SiC and SiCNWs. When the system energy supply during MTS pyrolysis is insufficient, the reaction is easy to be oversaturated and the grown SiC tends to combine with SiC to reduce the dependence on supplied energy. The PyC interphase is not evenly covered on the SiCNWs as shown in Fig. 1(d). The exposed SiC with little covered PyC interphase becomes perfect deposition sites for MTS pyrolyzing and attaching, while the following pyrolyzed SiC matrix tends to grow on the fixed deposition sites and the apparent agglomeration of SiC can be found. Fig. 1(e, f) are the surface morphologies of the samples without and with PyC interphase after a long time CVI process. The porosities of Fig. 1(e, f) are 66.2% and 72.7%, respectively. Fig. 1(e) is surface morphology of the sample without interphase, generated SiC wraps the SiCNWs and the thickness of the *in-situ* generated SiC shell gradually increases which makes the sample denser and denser. While the sample with PyC interphase is shown in Fig. 1(f), the agglomerated SiC particles gradually grow up to contact each other and compact the sample. Even for a long time CVI process, there exists little SiC on the PyC interphase for that PyC interphase is not an optimal deposition site when the the reaction is oversaturated. Reducing temperature will exacerbate the oversaturation, and the reaction prefers depositing SiC on the exposed SiC surface to lower the energy required.

The deposition temperature shows a significant effect on the growth morphology of the SiC matrix. After a long time of CVI deposition, SiC matrix deposited at 950, 1030 and 1100 ℃ have porosities of 67.3%, 66.2% and 63.5%, respectively. As shown in Fig. 2, the SiC matrix tends to preferentially grow into spherical particles when the temperature is lower than 950 ℃, while transforms into a hexagonal pyramidal when the temperature rises to 1030 ℃. Subsequently, the hexagonal pyramidal SiC matrix is still dominated when the temperature rises to 1100 ℃, but its particle size is significantly larger than that of the matrix deposited at 1030 ℃. Generally, the reaction temperature is an important parameter affecting the growth morphology, which is associated with reaction activity and energy. The pyrolysis of the precursor and the *in-situ* growth of the SiC matrix are processes of nucleation and re-growth, and the volume energy and surface energy are major factors to be considered. For the growth of the SiC matrix, the energy required as follows:

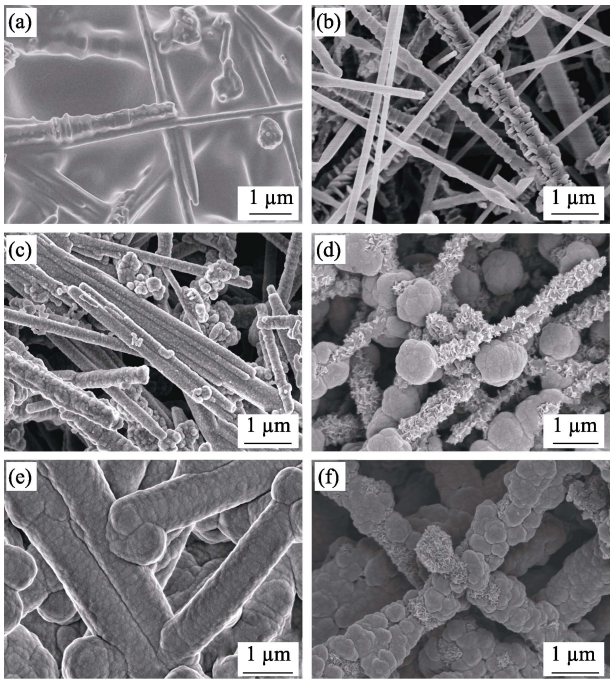

Fig. 1　Surface morphologies of the SiCNWs/PVA film (a), SiCNWs network without PyC and SiC deposition (b), surface morphologies of sample without (c) and with (d) PyC interphase after short time CVI process, and without (e) and with (f) PyC interphase after a long time CVI process

$$\Delta G=\left(\frac{4\pi r^3}{3}\right)\Delta G_{\mathrm{V}}+4\pi r^2\sigma \tag{1}$$

$$\text{Hemispherical particles: } \frac{d_v}{d_s}=\frac{r}{2} \tag{2}$$

$$\text{Cone particles: } \frac{d_{v_1}}{d_{s_1}}=\frac{r}{2}\sin\theta \tag{3}$$

where ΔG is the total energy required for SiC deposition, ΔG_{V} is the volume energy of SiC, σ is the surface

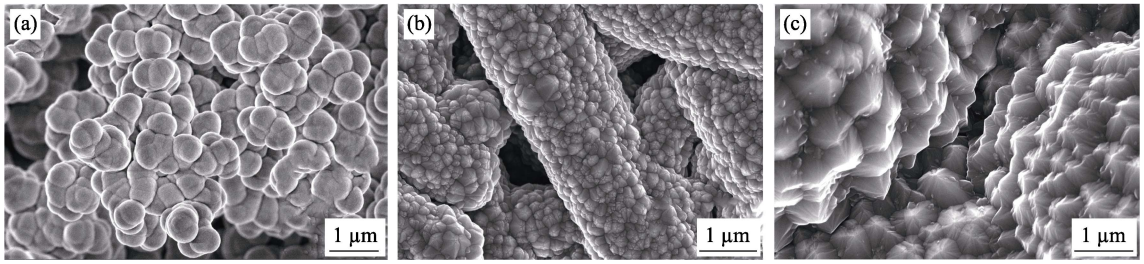

Fig. 2 Growth morphologies of SiC matrix CVI deposited at temperatures of (a) 950 ℃, (b) 1030 ℃, and (c) 1100 ℃

energy of SiC. *v* and *S* are the volume and surface of the grown SiC, respectively. In previous research, there are two growth morphologies of the grown SiC matrix obtained by the CVI process, including spherical and hexagonal cone shape[29]. Under the same growth conditions, the growth of the hexagonal cone shape requires the highest surface energy, while the growth of a spherical shape requires the lowest surface energy[30]. Therefore, at low temperature, the SiC matrix tends to preferentially grow into a spherical shape to reduce the energy required, which can be attributed to the insufficient system energy supply. When the temperature rises, the reaction is not over-saturated, and the spherical SiC matrix deposition can transform into hexagonal cone deposition. Moreover, the SiC matrix can also be deposited at the angle between the surfaces of two crystal grains to reduce the energy. So 1030 ℃ is chosen as the deposition temperature for the following pore parameter control.

The external surface and fracture surface morphologies of the prepared SiCNWs/SiC ceramic matrix composites with various deposition temperatures are shown in Fig. 3. The surfaces of the samples deposited at 1030 and 1100 ℃ show dense and little open pores, indicating that the continuous CVI process makes no effort for internal pore filling. As shown in Fig. 3(d), the more convex SiC spheres can be attributed to the temperature increase that accelerates the pyrolysis of the precursor, and consequently, the SiC matrix grows directly on the surface of the sample. The cross-section views in Fig. 3(b, e) demonstrate that the sample CVI deopsited at 1030 ℃ is denser than that deopsited at 1100 ℃, in which the layer thickness of grown SiC matrix is (267±33) and (125±27) nm, respectively. The porosity of the samples CVI deopsited at 1100 ℃ shows a porosity of 45.8%, compared with the one CVI deopsited at 1030 ℃ of 37.5%. Therefore, the increase in temperature increases the porosity and the densification difference between surface and internal. It can be explained by reaction kinetics that the movement of the precursor MTS in the horizontal direction is mainly determined by pumping force, whether it entered the internal pore of

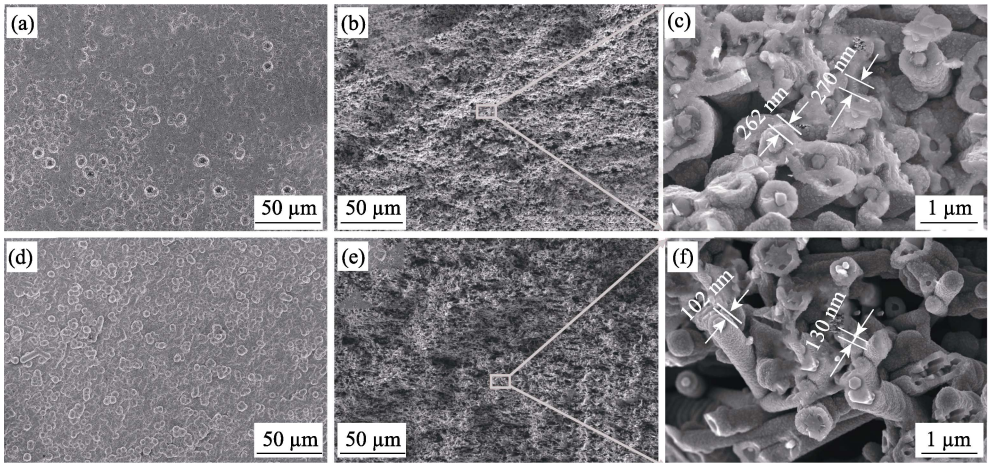

Fig. 3 SEM images of the prepared SiCNWs/SiC ceramic matrix composites

(a) External surface view of the sample under 8 h CVI process at 1030 ℃; (b) Fracture surface view and (c) corresponding enlarged region of the sample under 8 h CVI process at 1030 ℃; (d) External surface view of the sample under 8 h CVI process at 1100 ℃; (e) Fracture surface view and (f) corresponding enlarged region of the sample under 8 h CVI process at 1100 ℃

the SiCNWs network is influenced by molecular thermal movement. So it caters to Arrhenius formula[31]:

$$\frac{t_2}{t_1}=\frac{K_1}{K_2} \tag{4}$$

$$K=e^{\frac{-E_a}{RT}} \tag{5}$$

$$V=\sqrt{\frac{8kT}{\pi m}} \tag{6}$$

$$\frac{L_2}{L_1}=\frac{V_2t_2}{V_1t_1} \tag{7}$$

In which V_1 and V_2 are the average molecular thermal motion rates, K is the rate constant that represents the probability of pyrolysis per unit time, k is Boltzmann constant, E_a is the reaction activation energy, T is the temperature of the tube furnace, m is the molecular weight of MTS, t_2 and t_1 are the average thermal motion time of MTS before pyrolysis, L is the sum of thermal motion trajectory. V_1 approximately equals V_2, so $\frac{L_2}{L_1}=e^{\frac{-E_a}{R}\left(\frac{1}{T_1}-\frac{1}{T_2}\right)}$. Reducing temperature means more time left for the process that MTS fully decomposed into SiC, which is considered to that reducing reaction temperature can increase the pyrolysis time of MTS, thus extending the migration distance of MTS and increasing the chance for MTS to enter the internal channel. However, excessively lowering the temperature may change the growth state of the SiC matrix, or generate easily oxidized free silicon, which will eventually affect the performance of the ceramic matrix composites[32-36]. So 1030 ℃ is chosen as the deposition temperature for the following control of pore parameter, which can reduce the densification difference between surface and internal and improve the density of the composite.

The distributions of the pore sizes of the as-prepared SiCNWs/SiC ceramic matrix composites with different porosities is shown in Fig. 4. The *in-situ* deposited SiC wraps SiCNWs and the thickness of the deposited SiC shell increases. SiC can effectively fill the pores, and the pore size and porosity of the composites decrease. Besides, the proportion of small pores increases rapidly, which indicates that the big pores are filled into small pores. Compared with the sample with a porosity of 76.7% (volume percent), the sample with a porosity of 61.9% (volume percent) shows more small pores due to the greater slope. As the density increases, the volume fraction of small pores increases. Compared with the sample with a porosity of 38.9% (volume percent), the volume

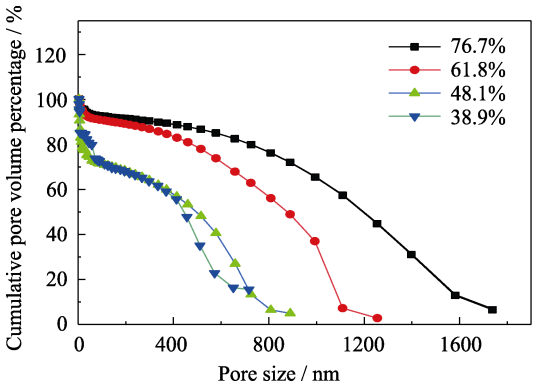

Fig. 4　Cumulative pore volume distribution with different pore size

fraction of small pores of the sample with a porosity of 48.1% (volume percent) is higher. With the densification increasing, the proportion of small pores decreases. The reason is that MTS molecules fail to flow through small pores and MTS molecules prefer to attach to the pore walls, which accelerates the blockage of the small pores, and the pores with small size decrease. The reduction of the small pores leads to the volume fraction of the small pores decreases dramatically. Therefore, the change of the pore structure can be monitored by the pore parameters.

The porous structure shows a significant impact on the strength and thermal conductivity of the as-prepared SiCNWs/SiC ceramic matrix composites. As shown in Fig. 5, the biaxial bending strength increases with the decrease of the porosity. The *in-situ* grown SiC wraps the SiCNWs, which results in the thickness of the *in-situ* generated SiC shell increasing and gradually making the network form a whole, and loading can effectively transfer between SiCNWs. The SiC deposition effectively enhances the connection of SiCNWs. The improvement of the strength increases as the amount of *in-situ* grown SiC increases, and the reason is that pore size can be treated as the size of the crack, and the reduction of the pore size is more meaningful for the strength improvement in the later stage. While the improvement of porosity on thermal conductivity decreases as the porosity decreases. The reason is that the thermal conductivity of the composite mainly depends on the heat conduction of the internal SiCNWs. In the early stage of the CVI process, SiC deposited at the cross-links of the SiCNWs, which enhanced the heat conduction between SiCNWs, and the thermal conductivity of the composite increases. As the thickness of the deposited SiC shell increase, the cross-section of the heat conduction channel increases. The heat transfer effect of SiC is less than that

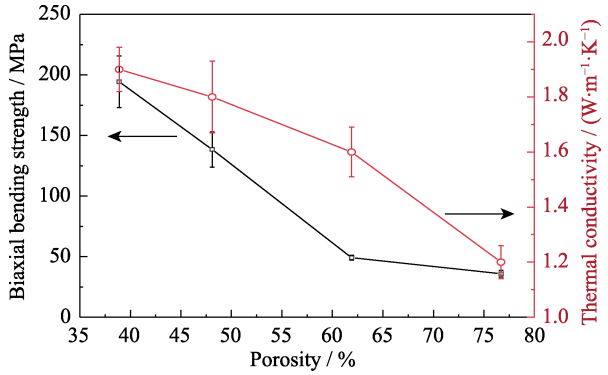

Fig. 5 Changes of strength and thermal conductivity with porosity of porous SiCNWs/SiC ceramic matrix composite

of SiCNWs, therefore the improvement of thermal conductivity decreases in the later stage of deposition. Compared with thermal conductivity, strength is more sensitive to the decrease of porosity. By adjusting the deposition temperature, the densification difference between surface and internal reduces, and the pore size of the composite reduces. Through optimizing pores parameter, the porous SiCNWs/SiC ceramic matrix composite with small size pore hopes a high strength. Through introducing PyC interphase into SiCNWs/SiC ceramic matrix composite, the composite shows a good mechanical enhancement effect. By introducing SiCNWs into the SiC matrix, the strength of the SiCNWs/SiC composite significantly improves. The performance and parameters of other porous materials are compared in Table 1. Comprehensive consideration of the strength and thermal conductivity, the composite of this work shows high strength and low thermal conductivity, and the SiCNWs/ SiC ceramic matrix composite with a porosity of 38.9% presents a strength of (194.3±21.3) MPa and a thermal conductivity of (1.9±0.1) W/(m·K).

Fig. 6 is the biaxial bending strength of the porous SiCNWs/SiC ceramic matrix with/without PyC interphase. The composite without interphase shows a strength of (138.5±14.7) MPa，and the composite with PyC interphase shows a higher strength of (194.3±21.3) MPa. Through introducing PyC interphase into SiCNWs/SiC ceramic matrix composite, the strength increased by 40.3%.

The section morphologies of the two samples with/without PyC interphase are shown in Fig. 7. The porosity of the composites with or without PyC interphase are all about 38%. As for the specimen with PyC interphase, there exists a longer pull-out length of SiCNWs on the fracture surface, and the fracture shows a certain cut angle compared with the flat fracture of the sample without PyC interphase. The moderate bonding strength between PyC interphase and SiC matrix and SiCNWs makes the nanowires easy debonded and pulled out from the matrix. The extended propagation path of the crack and the increased pull-out length of the nanowire demonstrated that more energy absorbed during the fracture process and PyC interphase contributes to the enhancement effect of SiCNWs even in the porous composite.

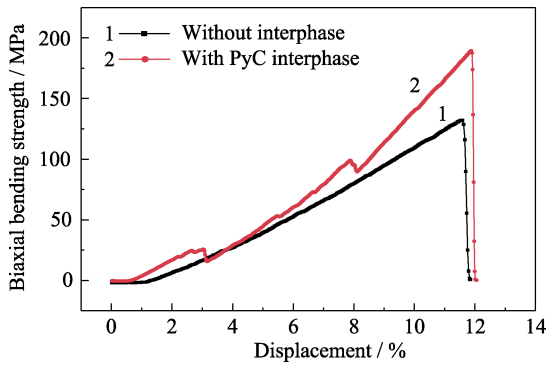

Fig. 6 Biaxial bending strength of the SiCNWs/SiC ceramic matrix composite with or without PyC interphase

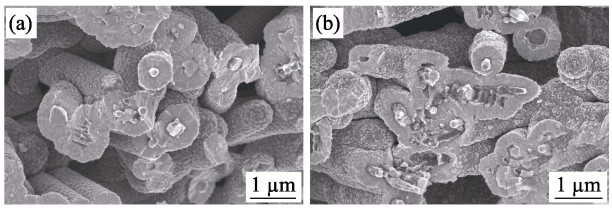

Fig. 7 Fracture morphologies of the SiCNWs/SiC ceramic matrix composite
(a) Without interphase; (b) With PyC interphase

Table 1 Strength and thermal conductivity of different materials

Material	Porosity/%	Strength /MPa	Thermal conductivity/(W·m^{-1}·K^{-1})	Ref.
Porous SiC-SiO_2 ceramic	~72	~2.7	0.066	[37]
Sc-doped porous SiC ceramic	~61	10.5	7.700	[38]
Porous Al_2O_3-SiC	~38	28.0	–	[39]
Porous ZrB_2-SiC ceramics	~59	~78.0	–	[40]
Porous SiC ceramic	~40	~10.7	0.580	[41]
Porous SiCNWs/SiC ceramic matrix composite	~39	~194.3	1.900	This work
Porous SiCNWs/SiC ceramic matrix composite	~62	~49.0	1.600	This work

3 Conclusion

The porous SiCNWs network framework with a volume fraction of 15.6% was prepared by mixing SiCNWs and PVA colloids. Through controlling CVI parameters to change the chemical reaction dynamics, two different *in-situ* grown SiC micro morphologies were obtained. Under different chemical reaction kinetics, the density and pore structure parameters of the porous SiCNWs/SiC ceramic matrix composite are also very different. The SiCNWs/SiC ceramic matrix composite with a porosity of 38.9% possesses thermal conductivity of (1.9±0.1) W/(m·K) and biaxial bending strength of (194.3±21.3) MPa.

Reference:

[1] LI S, ZENG X, CHEN H, *et al.* Porous hexagonal boron nitride nanosheets from g-C_3N_4 templates with a high specific surface area for CO_2 adsorption. *Ceramics International*, 2020, **46(17):** 27627–27633.

[2] SARAVANAN S, CHIDAMBARAM R K, GEO V E. An experimental study to analyze influence of porous media combustor on performance and emission characteristics of a DI diesel engine. *Fuel*, 2020, **280:** 118645–1–8.

[3] BICY K, KALARIKKAL N, STEPHEN A M, *et al.* Facile fabrication of microporous polypropylene membrane separator for lithium-ion batteries. *Materials Chemistry and Physics,* 2020, **255:** 123473–1–9.

[4] PAN B, CHEN J, ZHANG F, *et al.* Porous TiO_2 aerogel-modified SiC ceramic membrane supported MnO_x catalyst for simultaneous removal of NO and dust. *Journal of Membrane Science*, 2020, **611:** 118366–1–10.

[5] SONG X, JIAN B, JIN J. Preparation of porous ceramic membrane for gas-solid separation. *Ceramics International*, 2018, **44(16):** 20361–20366.

[6] WANG Z, PAN Z. Preparation of hierarchical structured nano-sized/ porous poly (lactic acid) composite fibrous membranes for air filtration. *Applied Surface Science*, 2015, **356:** 1168–1179.

[7] LIU X, MARTIN C L, BOUVARD D, *et al.* Strength of highly porous ceramic electrodes. *Journal of the American Ceramic Society*, 2011, **94(10):** 3500–3508.

[8] HUO W, ZHANG X, CHEN Y, *et al.* Mechanical strength of highly porous ceramic foams with thin and lamellate cell wall from particle-stabilized foams. *Ceramics International*, 2018, **44(5):** 5780–5784.

[9] SAUCEDO M L, LOWE T, ZHAO S, *et al. In situ* observation of mechanical damage within a SiC-SiC ceramic matrix composite. *Journal of Nuclear Materials*, 2016, **481:** 13–23.

[10] SONG C, LIU X, YE F, *et al.* Mechanical and dielectric properties of SiC_f/BN/SiBCN composites *via* different synthesis technologies. *Journal of the European Ceramic Society*, 2019, **39(14):** 4417–4423.

[11] WANG H, ZHOU X, YU J, *et al.* Fabrication of SiC_f/SiC composites by chemical vapor infiltration and vapor silicon infiltration. *Materials Letters*, 2010, **64(15):** 1691–1693.

[12] WONG E W, SHEEHAN P E, LIEBER C M. Nanobeam mechanics: elasticity, strength, and toughness of nanorods and nanotubes. *Science*, 1997, **277(5334):** 1971–1975.

[13] ZHANG Y, HAN X, ZHENG K, *et al.* Direct observation of superplasticity of beta-SiC nanowires at low temperature. *Advanced Functional Materials*, 2007, **17(17):** 3435–3440.

[14] VIVEKCHAND S R C, RAMAMURTY U, RAO C N R. Mechanical properties of inorganic nanowire reinforced polymer-matrix composites. *Nanotechnology*, 2006, **17(11):** 344–S350.

[15] XIN L, YANG W, ZHAO Q, *et al.* Strengthening behavior in SiC nanowires reinforced pure Al composite. *Journal of Alloys and Compounds*, 2017, **695:** 2406–2412.

[16] SHEN Q L, LI H J, LI L, *et al.* SiC nanowire reinforced carbon/ carbon composites with improved interlaminar strength. *Materials Science and Engineering*: *A*, 2016, **651:** 583–589.

[17] DONG L H, ZHANG H J, ZHANG J, *et al.* Carbon nanotube modified sepiolite porous ceramics for high-efficient oil/water separation. *Journal of Inorganic Materials*, 2020, **35(6):** 689–696.

[18] ZHANG K J, YADAV A, KIM K H, *et al.* Thermal and electrical transport in ultralow density single-walled carbon nanotube networks. *Advanced Materials*, 2013, **25(21):** 2926–2931.

[19] ZHAO X, HUANG C, LIU Q, *et al.* Thermal conductivity model for nanofiber networks. *Journal of Applied Physics*, 2018, **123(8):** 085103–1–10.

[20] MA R, CHENG X, YE W. SiC fiber and yttria-stabilized zirconia composite thick thermal barrier coatings fabricated by plasma spray. *Applied Surface Science*, 2015, **357:** 407–412.

[21] ZHUANG L, FU Q G, LIU T Y, *et al. In-situ* PIP-SiC NWs-toughened SiC-$CrSi_2$-Cr_3C_2-$MoSi_2$-Mo_2C coating for oxidation protection of carbon/carbon composites. *Journal of Alloys and Compounds*, 2016, **675:** 348–354.

[22] CHU Y, LI H, FU Q, *et al.* Toughening by SiC nanowires in a dense SiC-Si ceramic coating for oxidation protection of C/C composites. *Journal of the American Ceramic Society*, 2012, **95(11):** 3691–3697.

[23] WANG D, XUE C, BAI H, *et al.* Silicon carbide nanowires grown on graphene sheets. *Ceramics International*, 2015, **41(4):** 5473–5477.

[24] NGUYEN V H, DELBARI S A, AHMADI Z, *et al.* Electron microscopy characterization of porous ZrB_2-SiC-AlN composites prepared by pressureless sintering. *Ceramics International*, 2020, **46(16):** 25415–25423.

[25] LI X, YAO D, ZUO K, *et al.* Microstructure and permeability of porous YSZ ceramics fabricated by freeze casting of oil-in-water suspension. *Journal of the European Ceramic Society*, 2020, **40(15):** 5845–5851.

[26] FITZER E, HEGEN D. Chemical vapor-deposition of silicon-carbide and silicon-nitride-chemistrys contribution to modern silicon ceramics. *Angewandte ChemieInternational Edition*, 1979, **18(4):** 295–304.

[27] NASLAIN R, ROSSGNOL J Y, HAGENMULLER P, *et al*. Synthesis and properties of new composite-materials for high-temperature applications based on carbon-fibers and C-SiC or C-TiC hybrid matrices. *Revue De ChimieMinerale*, 1981, **18(5):** 544–564.

[28] RUAN J, YANG J S, DONG S M, *et al.* Interfacial optimization of SiC nanocomposites reinforced by SiC nanowires with high volume fraction. *Journal of the American Ceramic Society,* 2019, **102(9):** 5033–5037.

[29] ZHU Y, ZHANG Y, YAN L S. Interface between multi-layered

CVD SiC coating and its graphite substrate. *Equipment Environmetal Engineering*, 2019, **16(10):** 59–63.
[30] CHIN J, GANTZEL P K, HUDSON R G. The structure of chemical vapor deposition sillicon carbide. *Thin Solid Films*, 1977, **40:** 57–72.
[31] MASLOV M M, OPENOV L A, PODILIVAEV A I. On the vineyard formula for the pre-exponential factor in the Arrhenius law. *Physics of the Solid State*, 2014, **56(6):** 1239–1244.
[32] TIEGS T N. Fission product Pd-SiC interaction in irradiated coated-particle fuels. *Nuclear Technology*, 2017, **57(3):** 389–398.
[33] KINGON A I, LUTZ L J, LIAW P, *et al.* Thermodynamic calculations for the chemical vapor deposition of silicon carbide. *Journal of the American Ceramic Society*, 1983, **66(8):** 558–566.
[34] KAZUO M, KOUSAKU F. Structure of chemically vapour deposited silicon carbide for coated fuel particles. *Journal of Materials Science*, 1998, **23:** 699–706.
[35] BYUNG J C, DONG W P, DAI R K. Chemical vapour deposition of silicon carbide by pyrolysis of methylchlorosilanes. *Journal of Materials Science Letters*, 1997, **16:** 33–36.
[36] HAN D Y, MEI H, XIAO S S, *et al*. Porous SiC_{nw}/SiC ceramics with unidirectionally aligned channels produced by freeze-drying and chemical vapor infiltration. *Journal of the European Ceramic Society*, 2017, **37(3):** 915–921.
[37] KANG E S, KIM Y W, NAM H. Multiple thermal resistance induced extremely low thermal conductivity in porous SiC-SiO_2 ceramics with hierarchical porosity. *Journal of the European Ceramic Society*, 2021, **41(2):** 1171–1180.
[38] KULTAYEVA S, KIM Y W, SONG I H. Effects of dopants on electrical, thermal, and mechanical properties of porous SiC ceramics. *Journal of the European Ceramic Society*, 2021, **41(7):** 4006–4015.
[39] DEY A, KAYAL N, CHAKRABARTI O, *et al*. Studies on processing of layered oxide-bonded porous SiC ceramic filter materials. *International Journal of Applied Ceramic Technology*, 2021, **18(3):** 869–879.
[40] QI Y S, JIANG K, ZHOU C L, *et al*. Preparation and properties of high-porosity ZrB_2-SiC ceramics by water-based freeze casting. *Journal of the European Ceramic Society*, 2021, **41(4):** 2239–2246.
[41] RAJPOOT S, HA J H, KIMY W. Effects of initial particle size on mechanical, thermal, and electrical properties of porous SiC ceramics. *Ceramics International*, 2021, **47(6):** 8668–8676.

碳化硅纳米线增强多孔碳化硅陶瓷基复合材料的制备

阮 景[1,2,3], 杨金山[1,2], 闫静怡[1,2,4], 游 潇[1,2,4], 王萌萌[1,2,4],
胡建宝[1,2], 张翔宇[1,2], 丁玉生[1,2], 董绍明[1,2,5]

(1. 中国科学院 上海硅酸盐研究所 高性能陶瓷和超微结构国家重点实验室, 上海 200050; 2. 中国科学院 上海硅酸盐研究所 结构陶瓷及复合材料工程研究中心, 上海 201899; 3. 上海科技大学 物质科学与技术学院, 上海 201210; 4. 中国科学院大学, 北京 100039; 5. 中国科学院大学 材料科学与光电工程中心, 北京 100049)

摘 要: 构建多孔碳化硅纳米线(SiCNWs)网络并控制化学气相渗透(CVI)过程，可设计并获得轻质、高强度和低导热率 SiC 复合材料。首先将 SiCNWs 和聚乙烯醇(PVA)混合，制备具有最佳体积分数(15.6%)和均匀孔隙结构的 SiCNWs 网络；通过控制 CVI 参数获得具有小而均匀孔隙结构的 SiCNWs 增强多孔 SiC(SiCNWs/SiC)陶瓷基复合材料。SiC 基体形貌受沉积参数(如温度和反应气体浓度)的影响，从球状颗粒向六棱锥颗粒形状转变。SiCNWs/SiC 陶瓷基复合材料的孔隙率为 38.9%时，强度达到(194.3±21.3) MPa，导热系数为(1.9 ± 0.1) W/(m·K)，显示出增韧效果，并具有低导热系数。

关 键 词: SiC 基复合材料; 碳化硅纳米线; CVI 参数; 孔隙率; 热导率

中图分类号: TQ174 **文献标志码**: A